THE JOURNAL OF BIOLOGICAL CHEMISTRY VOL. 290, NO. 46, pp. 27868–27879, November 13, 2015

Assembly of a Tyr^{122} Hydrophobic Cluster in Sarcoplasmic Reticulum Ca^{2+}-ATPase Synchronizes Ca^{2+} Affinity Reduction and Release with Phosphoenzyme Isomerization*

Received for publication, September 20, 2015, and in revised form, October 2, 2015 Published, JBC Papers in Press, October 6, 2015, DOI 10.1074/jbc.M115.693770

Kazuo Yamasaki[1], **Takashi Daiho, Stefania Danko, and Hiroshi Suzuki**

From the Department of Biochemistry, Asahikawa Medical University, Midorigaoka-Higashi, Asahikawa 078-8510, Japan

Background: Ca^{2+} transport by Ca^{2+}-ATPase includes phosphoenzyme isomerization with luminal Ca^{2+} release.
Results: Mutation of Leu^{119}, Tyr^{122}, or Ile^{179} in an interdomain hydrophobic cluster retards release relative to isomerization.
Conclusion: There is a transient Ca^{2+}-bound state and affinity reduction during release governed by cluster assembly.
Significance: Ca^{2+} release is a multistep process directed by head domain gathering on transmembrane helix M2.

The mechanism whereby events in and around the catalytic site/head of Ca^{2+}-ATPase effect Ca^{2+} release to the lumen from the transmembrane helices remains elusive. We developed a method to determine deoccluded bound Ca^{2+} by taking advantage of its rapid occlusion upon formation of $E1PCa_2$ and of stabilization afforded by a high concentration of Ca^{2+}. The assay is applicable to minute amounts of Ca^{2+}-ATPase expressed in COS-1 cells. It was validated by measuring the Ca^{2+} binding properties of unphosphorylated Ca^{2+}-ATPase. The method was then applied to the isomerization of the phosphorylated intermediate associated with the Ca^{2+} release process $E1PCa_2 \rightarrow E2PCa_2 \rightarrow E2P + 2Ca^{2+}$. In the wild type, Ca^{2+} release occurs concomitantly with *E*P isomerization fitting with rate-limiting isomerization ($E1PCa_2 \rightarrow E2PCa_2$) followed by very rapid Ca^{2+} release. In contrast, with alanine mutants of Leu^{119} and Tyr^{122} on the cytoplasmic part of the second transmembrane helix (M2) and Ile^{179} on the A domain, Ca^{2+} release in 10 μM Ca^{2+} lags *E*P isomerization, indicating the presence of a transient *E*2P state with bound Ca^{2+}. The results suggest that these residues function in Ca^{2+} affinity reduction in *E*2P, likely via a structural rearrangement at the cytoplasmic part of M2 and a resulting association with the A and P domains, therefore leading to Ca^{2+} release.

Sarco(endo)plasmic reticulum Ca^{2+}-ATPase (SERCA1a),[2] a representative member of P-type ion-transporting ATPases, catalyzes Ca^{2+} transport coupled with ATP hydrolysis (Fig. 1) (for recent reviews, see Refs. 1–3). The enzyme is activated by the binding of two cytoplasmic Ca^{2+} ions at the high-affinity transport sites (*E*2 to $E1Ca_2$, steps 1 and 2) and autophosphorylated at Asp^{351} with MgATP to form an ADP-sensitive phosphoenzyme (*E*1P, step 3), which reacts with ADP to regenerate ATP in the reverse reaction. Upon *E*1P formation, the two bound Ca^{2+} are occluded in the transport sites ($E1PCa_2$). The subsequent isomeric transition to the ADP-insensitive *E*2P form results in rearrangements of the Ca^{2+} binding sites to deocclude Ca^{2+}, open the release path, and reduce the affinity, therefore releasing Ca^{2+} into the lumen (steps 4 and 5). Finally, the Asp^{351}-acylphosphate in *E*2P is hydrolyzed to form a Ca^{2+}-unbound inactive *E*2 state (step 6).

The *E*P isomerization associated with luminal Ca^{2+} release is a key rate-limiting process and involves a large rotation of the A domain, its association with the P domain and the cytoplasmic part of M2, and an inclination of associated A and P domains and the connected helices M2/M1 and M4/M5 via a steric effect of a M1/M2 V-shaped body (4–20). These motions are coupled to a rearrangement of the transport sites. We have found previously that the hydrophobic association of Leu^{119}/Tyr^{122} on the cytoplasmic part of M2 with the A and P domains (Tyr^{122} hydrophobic cluster) is critical for formation of the Ca^{2+}-released *E*2P ground state structure, with hydrolytic ability at the catalytic site and a properly opened luminal Ca^{2+} release path with reduced affinity at the transport sites (16–18). The Tyr^{122} hydrophobic cluster is formed with residues on the cytoplasmic part of M2 (Tyr^{122}/Leu^{119}), A domain (Ile^{179}/Leu^{180}), P domain (Val^{705}/Val^{726}), and A/M3 linker (Ile^{232}), thereby producing a most compactly organized head in *E*2P. The postulated $E2PCa_2$ transient intermediate was successfully trapped in the Ca^{2+}-occluded state (before deocclusion) by elongation of the A/M1′ linker with a two- or four-glycine insertion. Consistently in this state, the Tyr^{122} hydrophobic cluster was shown to not yet be fully formed. The finding demonstrates the critical role of the strain in this linker, probably to effect inclination of the A and P domains and connected helices required for deocclusion and Ca^{2+} release (19, 20).

Further understanding of Ca^{2+} binding/release processes in the transport cycle and roles of residues involved, especially the dynamic key process $E1PCa_2 \rightarrow E2PCa_2 \rightarrow E2P + 2Ca^{2+}$, is hampered by an inability to determine and detect the bound but deoccluded Ca^{2+} in minute amounts of expressed wild type and mutants obtained from cultured cells. In this study, we developed a method to determine the bound Ca^{2+} in the non-phosphorylated state as well as in the phosphorylated state of

* This work was supported by Grants-in-Aid for Scientific Research (C) (to K. Y.) and (B) (to H. S.) from the Ministry of Education, Culture, Sports, Science, and Technology of Japan. The authors declare that they have no conflicts of interest with the contents of this article.
[1] To whom correspondence should be addressed: Dept. of Biochemistry, Asahikawa Medical University, Midorigaoka-Higashi, Asahikawa, 078-8510, Japan. Tel.: 81-166-68-2353; Fax: 81-166-68-2359; E-mail: kyamasak@asahikawa-med.ac.jp.
[2] The abbreviations used are: SERCA, sarcoplasmic reticulum Ca^{2+}-ATPase; TG, thapsigargin.

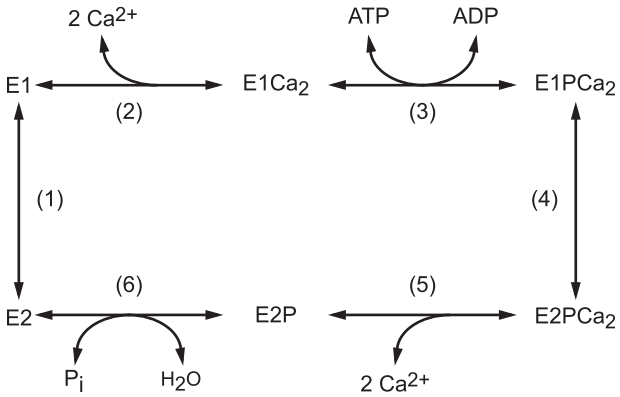

FIGURE 1. **Reaction schematic of Ca^{2+}-ATPase.**

expressed enzymes. We took advantage of the rapid occlusion in $E1PCa_2$ of bound Ca^{2+}, from either $E1Ca_2$ or $E2P$ species ($E2P$ and, possibly, the transient $E2P$ state with bound Ca^{2+}) by addition of a high concentration (10 mM) of Ca^{2+} (plus ATP for $E1Ca_2$) (21–25), probably trapping the bound Ca^{2+} before possible exchange with the added Ca^{2+}. The $E1PCa_2$ thus formed is very stable, probably because of Ca^{2+} substitution of Mg^{2+} bound at the catalytic Mg^{2+} subsite, as found previously (23, 26–29), therefore withstanding membrane filtration and extensive washing. We then applied this new method to the EP isomerization and Ca^{2+} release kinetic processes in alanine substitution mutants of the Tyr^{122} hydrophobic cluster because they are critical for the Ca^{2+}-released $E2P$ ground state structure (16–18). The results indicate the presence of a transient $E2P$ state with bound but deoccluded Ca^{2+} and show that Leu^{119} and Tyr^{122} on the cytoplasmic part of M2 and Ile^{179} on the A domain function via their association to reduce Ca^{2+} affinity during $E2P$ processing and, thereby, to accelerate Ca^{2+} release into the lumen. The detailed analyses suggest that a possibly stepwise assembly of the residues into the Tyr^{122} hydrophobic cluster takes place for proper Ca^{2+} handling (namely, deocclusion, affinity reduction, and release) and, therefore, Ca^{2+} transport coupled with EP processing.

Experimental Procedures

Mutagenesis and Expression—QuikChange™ site-directed mutagenesis (Stratagene) was utilized for the substitution of residues in rabbit SERCA1a cDNA. The ApaI-KpnI or KpnI-SalI restriction fragment was ligated back into the corresponding region in the full-length SERCA1a cDNA in the pMT2 expression vector (30). The pMT2 DNA was transfected into COS-1 cells with Lipofectamine and Plus™ reagent (Invitrogen), and the microsomes were prepared from COS-1 cells as described previously (18, 31).

Determination of EP—Microsomes expressing wild-type or mutant SERCA1a prepared from the COS-1 cells were phosphorylated with [γ-^{32}P]ATP or $^{32}P_i$ under the conditions described in the figure legends. The total amount of EP was determined following the addition of trichloroacetic acid. The amount of $E2P$ was determined by adding an equal volume of a solution containing 2 mM ADP and 5 mM EGTA, followed by the trichloroacetic acid addition 1 s after the ADP addition. The amount of EP was quantified with digital autoradiography after separation by 5% SDS-PAGE at pH 6.0 according to Weber and Osborn (32) and as described previously (33). The amount of EP in expressed SERCA1a was obtained by subtracting the background radioactivity determined in the absence of Ca^{2+}. In all mutants and the wild type, the background level was less than 1% of the total amount of EP.

Determination of Bound Ca^{2+}—Microsomes were incubated with 0–10 μM $^{45}Ca^{2+}$ at 4 °C in the absence or presence of 1 μM thapsigargin (TG), a highly specific and subnanomolar affinity inhibitor of SERCA that fixes the enzyme in the Ca^{2+}-unbound $E2$ state (34). 50 μl of reaction mixture was spotted on a membrane filter (Millipore, 0.45-μm mixed cellulose membrane HAWP) and washed for 3 s with 1 ml of Ca^{2+} binding assay medium containing 50 mM HEPES/Tris (pH 8.0), 0.1 M KCl, 10 mM $CaCl_2$, 7 mM $MgCl_2$, and 0.1 mM ATP. Other experimental conditions are described in detail in the figure legends. The $^{45}Ca^{2+}$ remaining on the filter was quantified by digital autoradiography. The amount of Ca^{2+} specifically bound to the Ca^{2+}-ATPase (trapped as occluded in $E1PCa_2$) was obtained by subtracting the amount of nonspecific Ca^{2+}-binding background determined in the presence of TG. We confirmed that all mutants retained TG sensitivity by observing that TG (1 μM used in this study) completely inhibits EP formation from [γ-^{32}P]ATP in the presence of Ca^{2+}, showing its validity for the background determination. The background level of nonspecific Ca^{2+} binding (in the presence of 10 μM Ca^{2+}) was ~100 pmol/mg of microsomal protein, which is 30–50% of total Ca^{2+} binding (see Fig. 4, *A* and *B*).

Miscellaneous—Protein concentrations were determined according to Lowry *et al.* (35). Data were analyzed by nonlinear regression using the program Origin (Microcal Software, Inc.). Free Ca^{2+} concentrations were calculated by the Calcon program. Three-dimensional models of SERCA1a were produced by the program VMD (36).

Results

Rapid $E1PCa_2$ Formation and Its Stabilization—To fix the bound Ca^{2+} in $E1Ca_2$ in an occluded form in $E1PCa_2$, it is necessary to rapidly phosphorylate $E1Ca_2$ to $E1PCa_2$ before Ca^{2+} release and to stabilize $E1PCa_2$ and prevent its decay during thorough washing. In analysis of the EP isomerization/Ca^{2+} release process $E1PCa_2 \rightarrow E2PCa_2 \rightarrow E2P + 2Ca^{2+}$, the $E2P$ species need to be rapidly converted to a stabilized $E1PCa_2$ state. The crucial feature for the forward reaction is to add a very high concentration (10 mM) of Ca^{2+} together with ATP. $E1PCa_2$ is extremely stable in a high concentration of Ca^{2+}, probably because of Ca^{2+} replacing catalytic subsite Mg^{2+}, as shown previously (23, 26–29). This stabilization prevents possible Ca^{2+} exchange at the transport sites in the reverse conversion in $E1PCa_2 \leftrightarrow E2P + 2Ca^{2+}$. Actually, the Mg^{2+} at the catalytic subsite is not "occluded" in $E1PCa_2$ and exchanges rapidly with Ca^{2+} at such a high concentration (26–28). Also, addition of a high concentration of Ca^{2+} rapidly converts $E2P$ to the stable $E1PCa_2$ in the reverse reaction (18, 22).

In Fig. 2*A*, wild-type SERCA1a expressed in microsomes of COS-1 cells was incubated with 10 μM Ca^{2+} to form the $E1Ca_2$ state in 7 mM Mg^{2+}, and then [γ-^{32}P]ATP plus an excess of EGTA or [γ-^{32}P]ATP plus 10 mM Ca^{2+} was added in 0.1 M KCl,

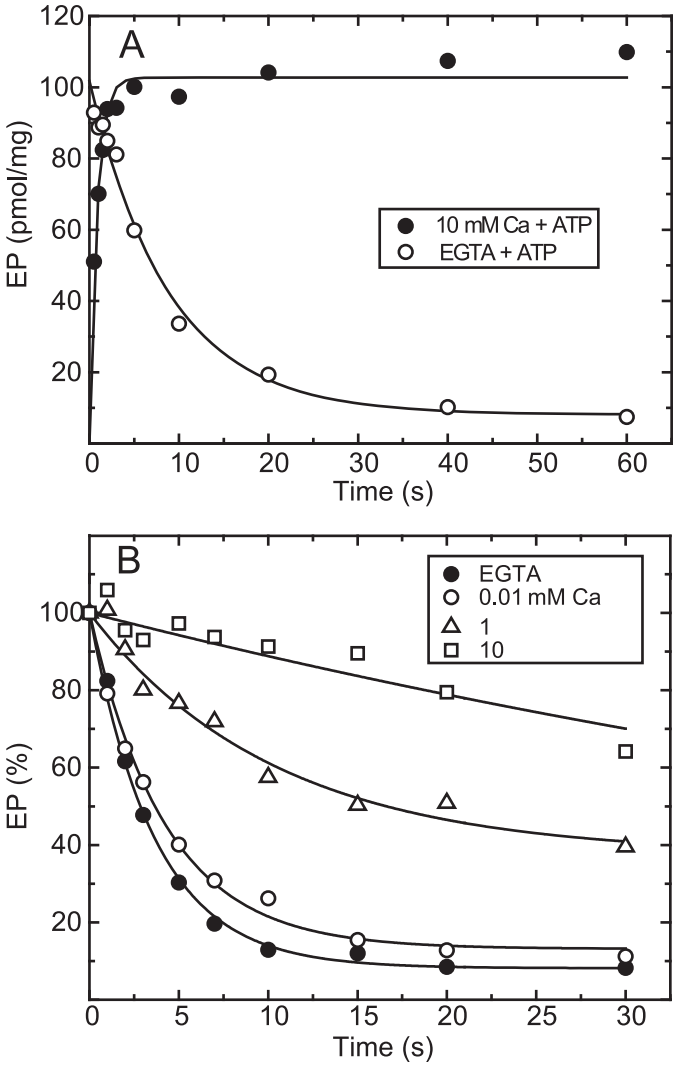

FIGURE 2. **Time course of *E*P formation and its decay in the wild type.** *A*, microsomes expressing wild-type Ca^{2+}-ATPase prepared from COS-1 cells were incubated with 10 μM Ca^{2+} in a mixture containing 20 μg/ml microsomal protein, 20 mM MOPS/Tris (pH 7.3), 0.1 M KCl, 7 mM $MgCl_2$, 10 μM $CaCl_2$, and 3 μM A23187 at 4 °C. Then *E*P formation was initiated at zero time by mixing with an equal volume of a solution containing 20 μM [γ-^{32}P]ATP, 0.1 M HEPES/Tris (pH 8.0), 0.1 M KCl, and 7 mM $MgCl_2$ with 10 mM $CaCl_2$ (*closed circles*) or 2 mM EGTA (*open circles*). *B*, *E*P was formed in 20 mM MOPS/Tris (pH 7.3), 0.1 M KCl, 7 mM $MgCl_2$, 10 μM $CaCl_2$, 3 μM A23187, and 10 μM [γ-^{32}P]ATP at 4 °C for 10 s. Then the reaction was chased at zero time by mixing with an equal volume of a solution containing non-radioactive 0.2 mM ATP and various concentrations of $CaCl_2$ to give the indicated final Ca^{2+} concentrations (0.01, 1, and 10 mM) or 2 mM EGTA to remove free Ca^{2+} in 0.1 M HEPES/Tris (pH 8.0), 0.1 M KCl, 7 mM $MgCl_2$, and 3 μM A23187. The amount of *E*P was normalized to the value at zero time of the chase.

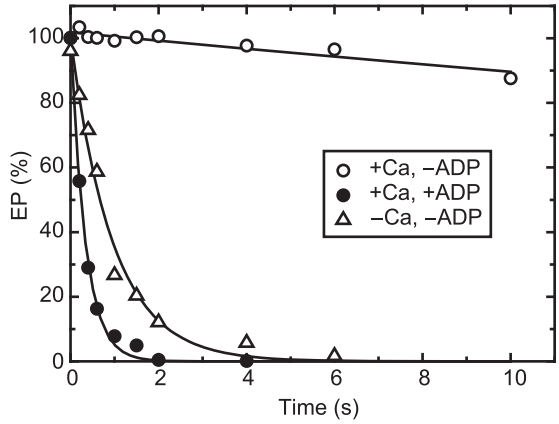

FIGURE 3. **Stabilization of *E*1PCa_2 formed by reverse conversion from *E*2P.** Wild-type Ca^{2+}-ATPase in microsomes was phosphorylated at 25 °C with 0.1 mM $^{32}P_i$ in a mixture containing 200 μg/ml microsomal protein, 50 mM MOPS/Tris (pH 7.3), 7 mM $MgCl_2$, 1 mM EGTA, 30 μM A23187, 7 mM $MgCl_2$, and 20% (v/v) Me_2SO that strongly favors *E*2P formation. The mixture was chilled at 4 °C and then, at zero time, diluted with a 19-fold volume of a solution containing 50 mM HEPES/Tris (pH 8.0), 0.105 M KCl, 7 mM $MgCl_2$, and 10.5 mM $CaCl_2$ (*open* and *closed circles*) or 1 mM EGTA (*open triangles*) in the absence (*open symbols*) or presence (*closed circles*) of 10.5 mM ADP, and the amount of *E*P was determined at the indicated times.

which accelerates *E*2P hydrolysis, causing *E*1PCa_2 accumulation (37). When ATP is added with EGTA, *E*1PCa_2 forms very rapidly despite the removal of free Ca^{2+} and then decays slowly via the rate-limiting *E*P isomerization, followed by rapid hydrolysis. The maximum *E*P level immediately after ATP/EGTA addition, estimated by an extrapolation of the single exponential decay to zero time, is very close to that obtained with ATP plus 10 mM Ca^{2+}. *E*1PCa_2 formation in 10 mM Ca^{2+} is also rapid and reaches a maximum within ~3 s, albeit slightly slower than that without free Ca^{2+} (*i.e.* with the substrate MgATP, consistent with previous kinetic studies (21–25)). Importantly, during this 3 s period, ~90% of *E*1PCa_2 remains when free Ca^{2+} is removed by EGTA. Therefore, *E*1PCa_2 formation and resulting Ca^{2+} occlusion by the simultaneous addition of ATP and 10 mM Ca^{2+} is rapid enough to trap almost all $^{45}Ca^{2+}$ originally bound in *E*1Ca_2 as an occluded *E*1PCa_2 species before Ca^{2+} release and possible $^{45}Ca^{2+}$-Ca^{2+} exchange (as demonstrated in Fig. 4).

In Fig. 2*B*, the decay of *E*1PCa_2 formed with [γ-^{32}P]ATP in 10 μM Ca^{2+} and 7 mM Mg^{2+} was initiated by a cold (non-radioactive) ATP chase in various concentrations of Ca^{2+}. The decay is slowed markedly with increasing Ca^{2+}. Actually, *E*1PCa_2 in 10 mM Ca^{2+} remains almost completely stable during the initial 3 s, a characteristic exploited in the Ca^{2+} binding assays in Figs. 4–10 as a period for membrane filter washing with 10 mM Ca^{2+}.

Rapid Luminal Ca^{2+}-induced Reverse Conversion E2P + $2Ca^{2+}$ → E2PCa_2 → E1PCa_2 and Stabilization of E1PCa_2—In Fig. 3, *E*2P was first formed with P_i and Mg^{2+} in the reverse reaction of hydrolysis, and then, at zero time, its decay was initiated by a large dilution with or without 10 mM Ca^{2+} in the presence of the Ca^{2+} ionophore A23187. When 10 mM Ca^{2+} is added, all *E*2P becomes stable *E*1P (as judged from its ADP sensitivity) because of Ca^{2+} binding to the luminally oriented, low-affinity Ca^{2+} transport sites (18, 22), in contrast to the rapid *E*2P hydrolysis without Ca^{2+} addition. The results show that *E*2P is very rapidly converted to *E*1PCa_2 upon addition of 10 mM Ca^{2+}, and *E*1PCa_2 thus formed is stabilized in 10 mM Ca^{2+}, in agreement with previous reports (23, 26–29). The results also suggest that *E*2P with bound Ca^{2+} can be fixed in the stable *E*1PCa_2 by reverse conversion.

Ca^{2+} Binding to the Non-phosphorylated Wild Type—Considering all of these advantages of rapid formation and stabilization of *E*1PCa_2 by the simultaneous addition of high concentrations of Ca^{2+} (10 mM) and ATP, we first determined the bound but non-occluded Ca^{2+} in wild type *E*1Ca_2 by membrane filtration, as shown in Fig. 4, *top panel*. Microsomes containing expressed Ca^{2+}-ATPase were incubated with various concentrations of $^{45}Ca^{2+}$, spotted on a membrane filter, and

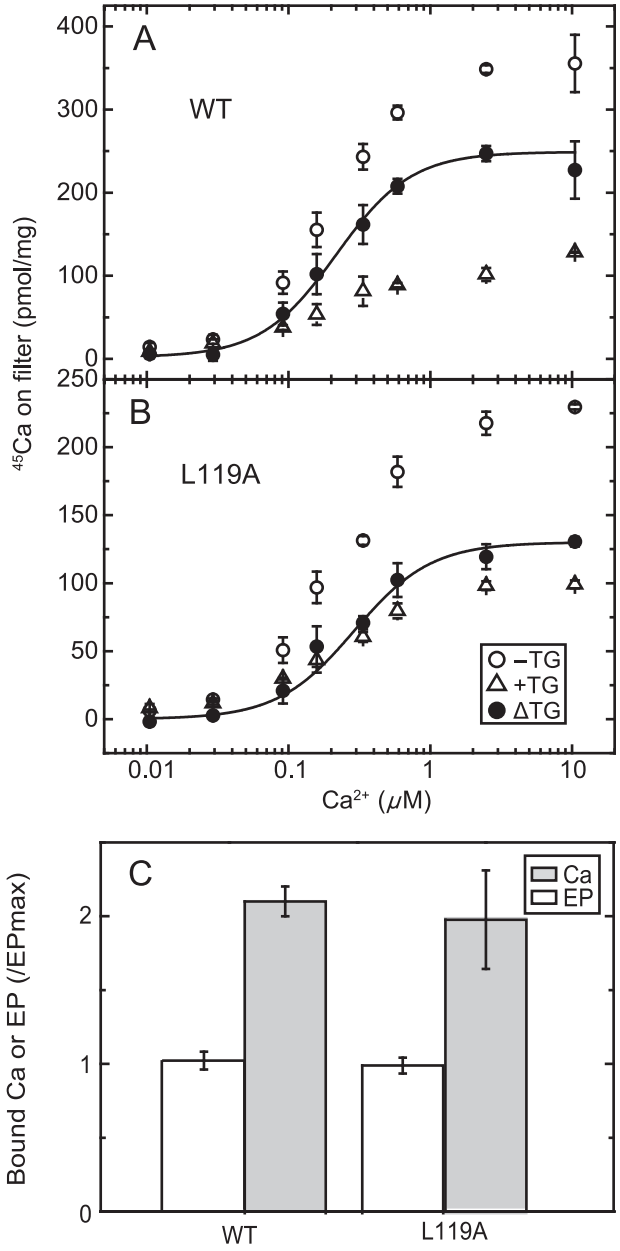

FIGURE 4. **Ca^{2+} concentration dependence of Ca^{2+} binding in non-phosphorylated Ca^{2+}-ATPase from COS-1 cells.** *A* and *B*, microsomes expressing the wild type (*A*) or mutant L119A (*B*) were incubated at 4 °C for 20 s with various concentrations of $^{45}Ca^{2+}$ in a mixture containing 20 μg/ml microsomal protein, 50 mM MOPS/Tris (pH 7.3), 0.1 M KCl, 7 mM $MgCl_2$, 3 μM A23187, and 10 μM $^{45}CaCl_2$ with 0–0.09 mM EGTA to give the indicated free Ca^{2+} concentration in the presence (*open triangles*) or absence (*open circles*) of 1 μM TG. Then, as described under "Experimental Procedures," 50 μl of the mixture was spotted on a membrane filter and washed immediately for 3 s with 1 ml of a Ca^{2+} binding assay medium containing 10 mM $CaCl_2$ and 0.1 mM ATP in 50 mM HEPES/Tris (pH 8.0), 0.1 M KCl, and 7 mM $MgCl_2$. The values presented are the mean ± S.D. (n = 3–4). The amount of Ca^{2+} specifically bound to the Ca^{2+}-ATPase (trapped as occluded Ca^{2+} in $E1PCa_2$, *closed circles*) was obtained by subtracting the amount of nonspecific Ca^{2+} binding determined in the presence of TG. The *solid lines* show the least squares fit to the Hill equation with the fitting parameters K_d and Hill coefficient of 0.22 μM and 1.6 for the wild type and 0.29 μM and 1.6 for the mutant L119A. *C*, the maximum amount of specific $^{45}Ca^{2+}$ binding in 10 μM $^{45}Ca^{2+}$ was determined as above (*Ca*) and compared with the maximum amount of *E*P (*EP*) determined in the presence of 10 mM Ca^{2+} as in Fig. 2*A* (*i.e.* essentially under the same conditions as described for the determination of the catalytic site content in the preparation (45)). It should be mentioned here that, for the comparison, one preparation of microsomes was used throughout for the wild type and the mutant. Actual values of the amount of bound Ca^{2+} and that of *E*P (pmol/mg of microsomal protein (n = 4)) for the wild type were 287 ± 14 and 136 ± 8, respectively, giving a stoichiometry of Ca/*E*P = 2.11. Those for the L119A mutant were 95.6 ± 16.2 and 48.6 ± 2.6, respectively, providing a stoichiometry of Ca/*E*P = 1.97. Note that these maximum Ca^{2+} binding values are slightly different from those in *A* and *B*, in which different preparations were used.

exposed to continuous washing with Ca^{2+} binding assay medium containing 0.1 mM ATP and 10 mM non-radioactive Ca^{2+} for 3 s, during which $E1PCa_2$ is rapidly formed and stabilized and free $^{45}Ca^{2+}$ is washed out. The amount of $^{45}Ca^{2+}$ specifically bound to the Ca^{2+}-ATPase was obtained by subtracting the background determined in the presence of TG from that in its absence. The $^{45}Ca^{2+}$ concentration dependence shows a saturation curve with a K_d value and Hill coefficient of 0.22 μM and 1.64, respectively, and a stoichiometry of maximum binding of ~2 Ca^{2+} per catalytic site (maximum amount of *E*P, Fig. 4*C*), in complete agreement with the properties of the high-affinity transport sites established with sarcoplasmic reticulum vesicle Ca^{2+}-ATPase (38) (whose values actually observed by this method are a K_d of 0.25 μM, a Hill coefficient of 1.61, and a stoichiometry of ~2). Therefore, this method clearly fixes the $^{45}Ca^{2+}$ originally bound in $E1Ca_2$ of expressed SERCA1a in an occluded form as $E1PCa_2$ before its release and exchange with the non-radioactive Ca^{2+} at 10 mM in the Ca^{2+} binding assay medium. This validates the method for measuring Ca^{2+} binding for small quantities of expressed SERCA1a.

The results also imply that there is virtually no exchange of the bound $^{45}Ca^{2+}$ in $E1PCa_2$ with the subsequently added 10 mM non-radioactive Ca^{2+}. As noted above, this is probably due to stabilization of $E1PCa_2$ by Ca^{2+} substituting for Mg^{2+} at the catalytic Mg^{2+} subsite (23, 26–29) rather than the Ca^{2+}-induced reverse conversion in the equilibrium $E1PCa_2 \leftrightarrow E2P + 2Ca^{2+}$, which would result in Ca^{2+} exchange at the transport sites. Notably, also, previous analyses of Ca^{2+} binding/release in non-phosphorylated enzyme $E1Ca_2 \leftrightarrow E2 + 2Ca^{2+}$ shows (39–41) that the Ca^{2+} bound at transport site II is exposed to the medium and exchangeable with medium Ca^{2+}, whereas Ca^{2+} bound at the deeply located site I is not released (unless site II becomes empty). ATP-induced phosphorylation to $E1PCa_2$ requires both Ca^{2+} to be bound. Our results indicate that $E1PCa_2$ formation upon addition of ATP and 10 mM Ca^{2+} is sufficiently fast to avoid such a Ca^{2+} exchange at site II, thereby trapping both of the $^{45}Ca^{2+}$ originally bound in the $E1Ca_2$ state as $E1PCa_2$.

Time Course of Ca^{2+} Release and EP Isomerization in the Wild Type—The Ca^{2+} binding assay was applied to analyze the *E*P isomerization and Ca^{2+} release process in the wild type (Fig. 5). The experiments were performed in the presence of 0.1 M KCl, in which *E*2P does not accumulate because of its rapid hydrolysis (37), and, therefore, the *E*P decay reflects rate-limiting $E1PCa_2$ isomerization to *E*2P (as shown in our previous report, *cf.* Fig. 2*A* in Ref. 42). In Fig. 5*B*, the expressed wild type was incubated with 10 μM $^{45}Ca^{2+}$ and phosphorylated with ATP to form $E1PCa_2$, and then an aliquot of the sample was placed on the membrane filter. At zero time, $E1PCa_2$ decay was initiated by removal of $^{45}Ca^{2+}$ by excess EGTA, and, after the indicated time periods, the sample was washed for 3 s with Ca^{2+} binding assay medium containing 10 mM non-radioactive

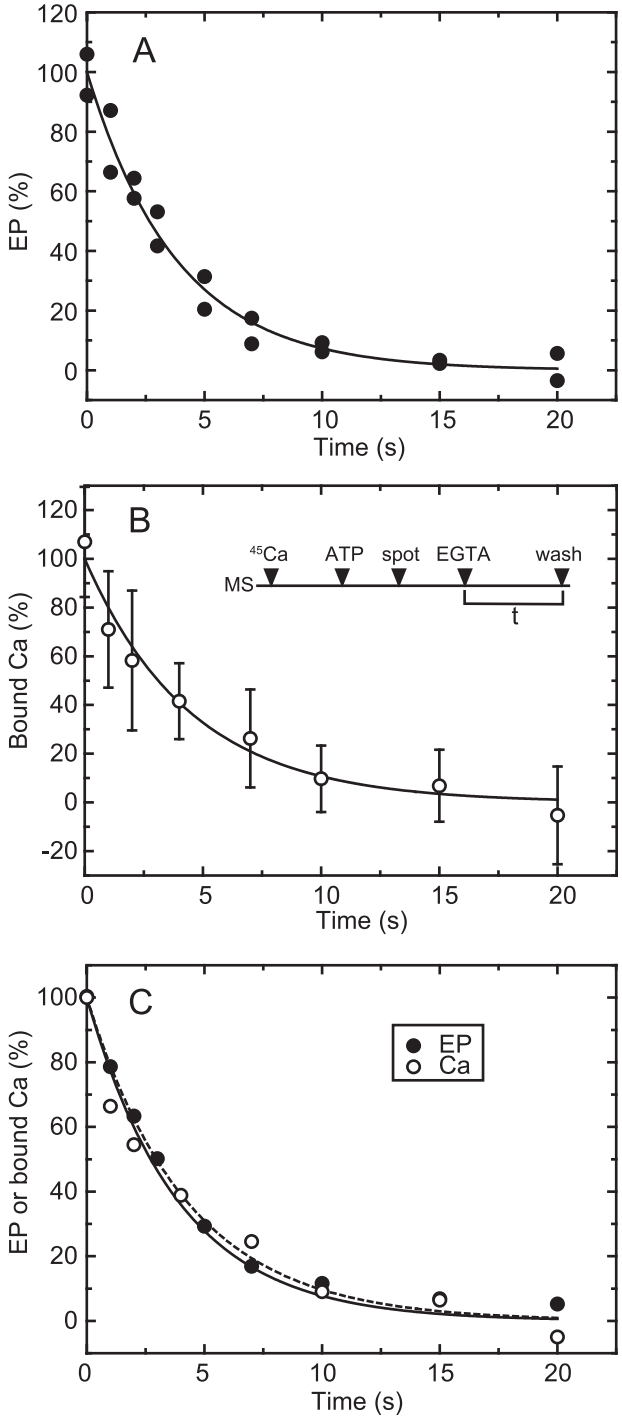

FIGURE 5. **Time courses of *E*P isomerization and Ca^{2+} release in the wild type.** *A*, for the determination of *E*P, wild-type Ca^{2+}-ATPase was phosphorylated in a mixture containing 20 μg/ml microsomal protein, 20 μM [γ-^{32}P]ATP, 10 μM $CaCl_2$, 50 mM MOPS/Tris (pH 7.3), 0.1 M KCl, 7 mM $MgCl_2$, and 3 μM A23187. Then the phosphorylation was chased at zero time by mixing with an equal volume of EGTA chase solution containing 1 mM EGTA, 50 mM MOPS/Tris (pH 7.3), 0.1 M KCl, 7 mM $MgCl_2$, and 3 μM A23187. The reaction was quenched by acid at the indicated times. Here it should be noted that nearly all the *E*P was *E*1P in the presence of KCl (actually more than 95%), as we observed under essentially the same conditions (*cf.* Fig. 2*A* in Ref. 42). Therefore, *E*P decay represents *E*P isomerization (which is followed by rapid *E*2P hydrolysis). *B*, for the Ca^{2+} binding assay, wild-type Ca^{2+}-ATPase in microsomes (*MS*) was incubated for 5 s with 10 μM $^{45}Ca^{2+}$ in 50 mM MOPS/Tris (pH 7.3), 0.1 M KCl, 7 mM $MgCl_2$, and 3 μM A23187 and phosphorylated by addition of a small volume of ATP to give 10 μM (*ATP*) for 20 s. Immediately, the mixture (50 μl) was spotted on the membrane filter (*spot*), and, at zero time (*EGTA*), free Ca^{2+} was removed to initiate *E*P decay by continuous rinsing with the above EGTA chase solution. After various periods (*t*), the amount of $^{45}Ca^{2+}$ specifically bound to Ca^{2+}-ATPase was determined by washing the filter with 1 ml of the Ca^{2+} binding assay medium as in Fig. 4 (*wash*). The values presented are the mean ± S.D. (n = 3–6). *C*, the time courses of *E*P decay (*closed circles*) and decrease in bound $^{45}Ca^{2+}$ (*open circles*) determined in *A* and *B* are replotted in the same panel. The plots show the mean values in *A* and *B*. The *solid* and *broken lines* show a single exponential fit in which the rates are 0.23 s^{-1} for *E*P decay and 0.22 s^{-1} for the decrease in bound $^{45}Ca^{2+}$, respectively.

Ca^{2+}. For the determination of *E*P, [γ-^{32}P]ATP and non-radioactive Ca^{2+} were used. The decrease in *E*P (representing *E*P isomerization) and that in bound Ca^{2+} coincide perfectly with the established mechanism in the wild type. The rate-limiting $E1PCa_2$ to $E2PCa_2$ isomerization is followed by the very rapid Ca^{2+} release $E2PCa_2 \rightarrow E2P + 2Ca^{2+}$. The results obtained by this method are also in complete agreement with those established with sarcoplasmic reticulum vesicles, which contain a large proportion of Ca^{2+}-ATPase, by the usual direct Ca^{2+} binding assay (*i.e.* without washing of the membrane filter) (42). Therefore, the Ca^{2+} release kinetics associated with *E*P isomerization can be followed by this assay using even small quantities of enzyme expressed in COS-1 cell microsomes.

Ca^{2+} Release in 10 μM Ca^{2+} Is Slower than EP Isomerization in the L119A Mutant—Detailed kinetic measurements of *E*P isomerization and Ca^{2+} release were made, first with the mutant L119A. We focused on residue Leu^{119} first because proteinase K-specific cleavage occurs at Leu^{119} in $E2PCa_2$ (*E*2P with occluded Ca^{2+} trapped by elongation of the A/M1′ linker) and its analog $E2{\cdot}BeF_3^-{\cdot}Ca_2$, but not in the Ca^{2+}-released *E*2P ground state and its analog $E2{\cdot}BeF_3^-$ (7, 19, 20), and Leu^{119} is critical in the *E*2P ground state with reduced Ca^{2+} affinity (18). We hypothesized that this residue on the cytoplasmic part of M2, possibly its gathering into the Tyr^{122} hydrophobic cluster, may be involved in Ca^{2+} release during *E*2P processing and Ca^{2+} release ($E2PCa_2 \rightarrow E2P + 2Ca^{2+}$). First, we found, as shown in Fig. 4*B*, that the properties of the Ca^{2+} binding sites of non-phosphorylated L119A (expression level about half of that of the wild type) are a K_d of 0.29 μM, a Hill coefficient of 1.61, and the stoichiometry 2 per one catalytic site (Fig. 4*C*), essentially the same as those of the wild type (*cf.* Fig. 4*A*). After establishing this stoichiometry of Ca^{2+} binding, we compared, in Fig. 6, the rate of Ca^{2+} release with that of *E*P isomerization.

In Fig. 6*A*, $E1Ca_2$ was formed with saturating 10 μM $^{45}Ca^{2+}$ and ionophore A23187, and phosphorylated at zero time to form $E1PCa_2$ by the addition of 10 μM ATP with and without excess EGTA, and then the sample was spotted on the membrane filter, otherwise as in Fig. 5*B*. $E1PCa_2$ is rapidly formed, and, as seen in Fig. 6*B*, there is almost no change in the total amount of *E*P during the time period because of the nearly complete block of *E*2P hydrolysis by the Leu^{119} mutation, whereas the *E*2P fraction increases gradually upon *E*P isomerization. When free $^{45}Ca^{2+}$ is removed by EGTA, $^{45}Ca^{2+}$ release takes place at the same rate as that of *E*2P formation. On the other hand, in the presence of 10 μM $^{45}Ca^{2+}$, $^{45}Ca^{2+}$ release is slower than *E*2P formation by ~2-fold as a result of *E*P isomerization. The results suggest that, in 10 μM Ca^{2+}, there may be a transient intermediate *E*2P state with bound Ca^{2+} at the transport sites with still a rather high affinity. Therefore, in this L119A mutant, Ca^{2+} affinity reduction at the transport sites

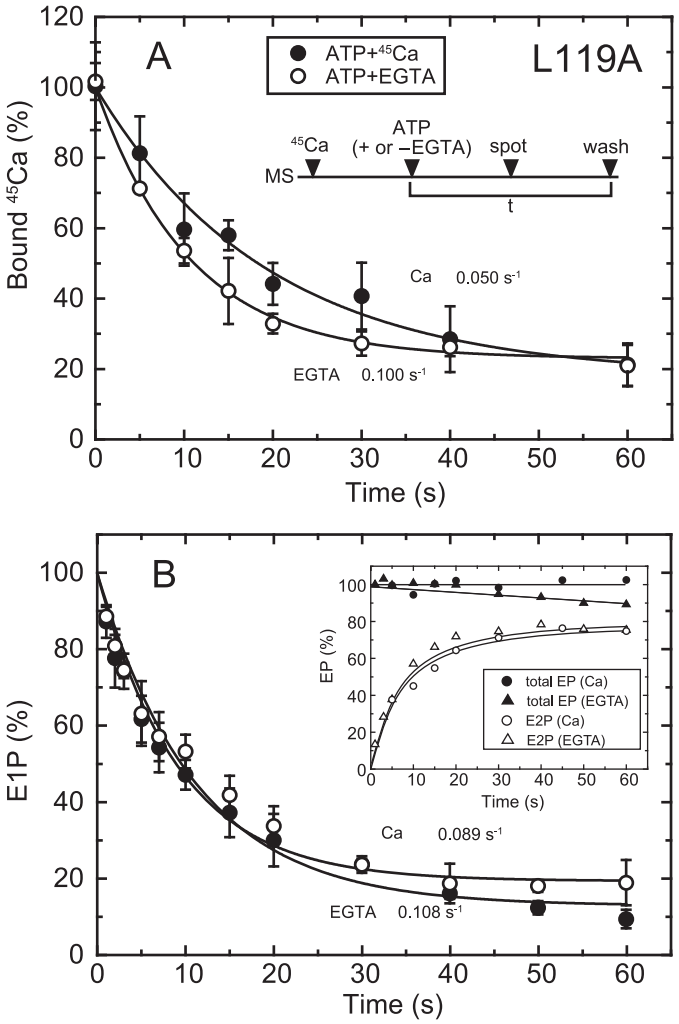

FIGURE 6. **Time courses of Ca^{2+} release and *EP* isomerization in mutant L119A.** *A*, microsomes (*MS*) expressing mutant L119A (20 μg/ml microsomal protein) were incubated for 20 s with 10 μM $^{45}Ca^{2+}$ in 50 mM MOPS/Tris (pH 7.3), 0.1 M KCl, 7 mM $MgCl_2$, and 3 μM A23187. Then, at zero time (*ATP + or −EGTA*), phosphorylation was initiated by addition of 10 μM ATP with (*open circles*) or without 1 mM EGTA (*closed circles*), the mixture was spotted on the filter, and the amount of $^{45}Ca^{2+}$ specifically bound to the Ca^{2+}-ATPase was determined as in Fig. 5*B*. The values presented are the mean ± S.D. (n = 3–5). The *solid lines* show a single exponential fit, and the rates of the $^{45}Ca^{2+}$ release thus determined are 0.10 s^{-1} in an excess of EGTA (*open circles*) and 0.05 s^{-1} in the presence of 10 μM $^{45}Ca^{2+}$ (*closed circles*). *B*, *inset*, microsomes expressing the mutant L119A (40 μg/ml microsomal protein) in 10 μM Ca^{2+} were phosphorylated at zero time by mixing with an equal volume of a solution containing 20 μM [γ-^{32}P]ATP and 10 μM $CaCl_2$ (*circles*) or 2 mM EGTA (*triangles*), and the total amount of *EP* (*closed symbols*) and the amount of *E*2P (*open symbols*) were determined at the indicated times as in Fig. 5*A*. *Main panel*, the fraction of *E*1P in the total amount of *EP* was calculated at each time point by subtracting the amount *E*2P from the total amount of *EP* (*E*1P plus *E*2P). The *solid lines* show a single exponential fit, and the rates of the decrease in *E*1P fraction, *i.e.* the *E*1P to *E*2P isomerization, thus determined are 0.108 s^{-1} in an excess of EGTA (*open circles*) and 0.089 s^{-1} in the presence of 10 μM Ca^{2+} (*closed circles*).

likely occurs after *EP* isomerization ($E1PCa_2 \rightarrow E2PCa_2$ at the catalytic site) and release gate opening, causing Ca^{2+} release to be retarded. Note that, for the wild type, this type of kinetic experiment in the presence of 10 μM Ca^{2+} is not feasible because, after Ca^{2+} release, $E1Ca_2$ is quickly regenerated upon rapid *E*2P hydrolysis to *E*2, followed by immediate Ca^{2+} rebinding. The results with the L119A mutant nevertheless suggest that some structural rearrangement takes place at the Leu^{119} region on the cytoplasmic part of M2, possibly formation of the Tyr^{122} hydrophobic cluster, to effect Ca^{2+} affinity reduction and release.

EP Isomerization and Ca^{2+} Release in other Tyr^{122} Hydrophobic Cluster Mutants—To further explore possible roles in the Ca^{2+} release process of other residues in the Tyr^{122} hydrophobic cluster, *i.e.* the hydrophobic interactions of the cytoplasmic part of M2 with the A and P domains and A/M3 linker (Leu^{119}/Tyr^{122} (M2), Ile^{179}/Leu^{180} (A), Val^{705}/Val^{726} (P), and Ile^{232} (A/M3 linker), see Fig. 11), we performed the same set of detailed kinetic measurements with mutant Y122A on the cytoplasmic part of M2 and I179A and V705A as representative for A and P domain interactions, respectively. It should be mentioned here that the stoichiometry of the maximum $^{45}Ca^{2+}$ binding in Y122A, I179A, and V705A (Ca/*E*P determined as in Fig. 4*C*) are 2.03, 1.72, and 2.18, respectively, very similar to those in L119A and the wild type (1.97 and 2.11, respectively, see the legend for Fig. 4). Furthermore, the K_d (μM) and Hill coefficient of the Ca^{2+} binding sites determined with the Ca^{2+} concentration dependence of $E1PCa_2$ formation from $E1Ca_2$ are also in essential agreement in these mutants and the wild type, showing respective values 0.31 and 1.93 (Y122A), 0.24 and 1.98 (I179A), 0.35 and 1.90 (L119A), 0.61 and 1.51 (V705A), and 0.29 and 1.91 (wild type) (see Table 1 in Ref. 17).

In Y122A, as in L119A, *E*2P hydrolysis was nearly completely blocked (17), and the single exponential *E*2P accumulation in *EP* isomerization was observed with the same rates in the presence and absence of 10 μM Ca^{2+} (Fig. 7*B*). The $^{45}Ca^{2+}$ release in 10 μM $^{45}Ca^{2+}$ occurs in a single exponential manner (Fig. 7*A*) and is slower than *E*2P formation by more than 2-fold. Therefore, in Y122A, as in L119A, Ca^{2+} release after *E*2P formation is retarded in 10 μM Ca^{2+}.

The $^{45}Ca^{2+}$ release in Y122A upon $^{45}Ca^{2+}$ removal by EGTA exhibits interesting kinetics. Immediately after removal, some portion of the bound $^{45}Ca^{2+}$ (~35% of the total, Fig, 7*A*, *open circles*) disappeared rapidly before formation of *E*2P (Fig. 7*B*, *inset*, *closed triangles*). The remaining part of the bound Ca^{2+} is released in a single exponential manner at the same rate as that of *E*2P formation in *EP* isomerization. This result suggests that the Ca^{2+}-occluded structure in $E1PCa_2$ is destabilized in this mutant so that a fraction of the Ca^{2+} of $E1PCa_2$ is released rapidly (without affinity reduction because such a rapid release does not occur in 10 μM Ca^{2+}). Similarly, we previously observed Ca^{2+} release (escape) from $E1PCa_2$ without affinity reduction in the wild type in the absence of K^+ and indicated that the stabilization of $E1PCa_2$, in this case by the K^+ binding on its specific site on the P domain, is crucial for stabilizing the Ca^{2+}-occluded structure of $E1PCa_2$ (42). Therefore, similar to the bound K^+, Tyr^{122} is likely important for the structural stabilization of $E1PCa_2$ with occluded Ca^{2+}.

In the alanine mutants of Ile^{179} and Val^{705} that form the Tyr^{122} hydrophobic cluster, *EP* decay occurs fairly fast because of the faster *E*2P hydrolysis, as found previously (16, 17) (Fig. 8, see the decay after the Ca^{2+} removal (*triangles*), although it is still much slower than the wild type (*cf.* Fig. 5)). Nevertheless, within the initial time period of ~20 s in the presence of 10 μM Ca^{2+}, during which the amount of original *EP* species remains significant, we were able to compare *E*2P formation and Ca^{2+}

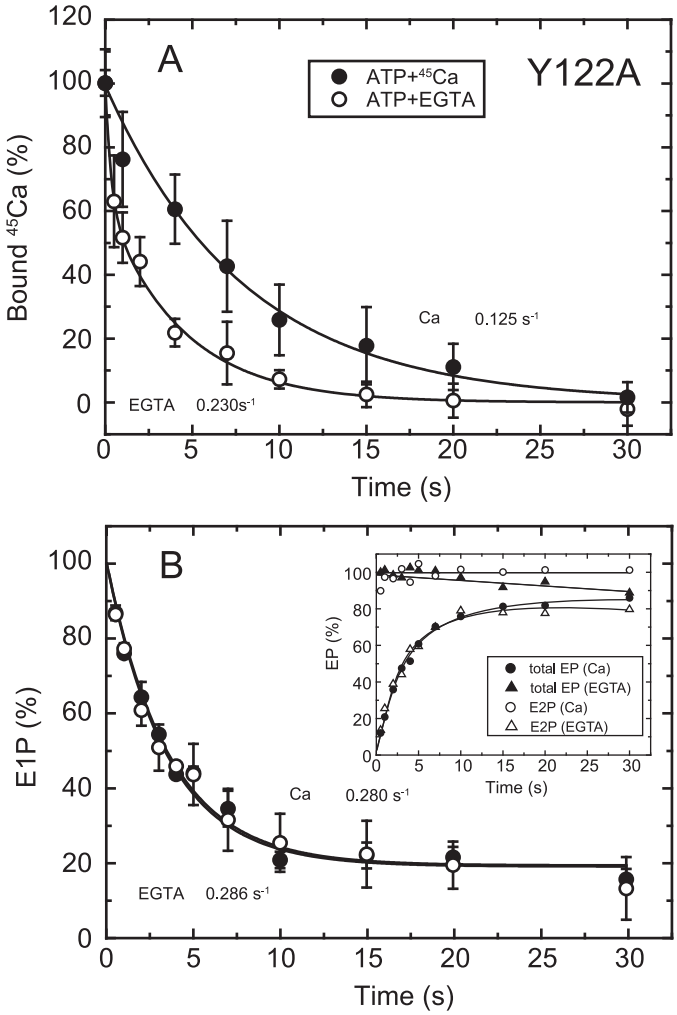

FIGURE 7. **Time courses of Ca^{2+} release and *EP* isomerization in mutant Y122A.** *A*, Ca^{2+} release from *E*P in the mutant Y122A was determined as in Fig. 6*A*. The values presented are the mean ± S.D. (n = 3–5). The *solid lines* show a single exponential fit, and the rates of the $^{45}Ca^{2+}$ release thus determined are 0.23 s^{-1} in an excess of EGTA (*open circles*) and 0.125 s^{-1} in the presence of 10 μM $^{45}Ca^{2+}$ (*closed circles*). *B*, *inset*, the total amount of *E*P (*closed symbols*) and the amount of *E*2P (*open symbols*) were determined at the indicated times with the mutant Y122A as described in Fig. 6*B*. *Main panel*, the fraction of *E*1P in the total amount of *E*P was calculated at each time point by subtracting the amount *E*2P from the total amount of *E*P (*E*1P plus *E*2P). The *solid lines* show a single exponential fit, and the rates of the decrease in *E*1P fraction, *i.e.* the *E*1P to *E*2P isomerization, thus determined are 0.286 s^{-1} in an excess EGTA (*open circles*) and 0.280 s^{-1} in the presence of 10 μM Ca^{2+} (*closed circles*).

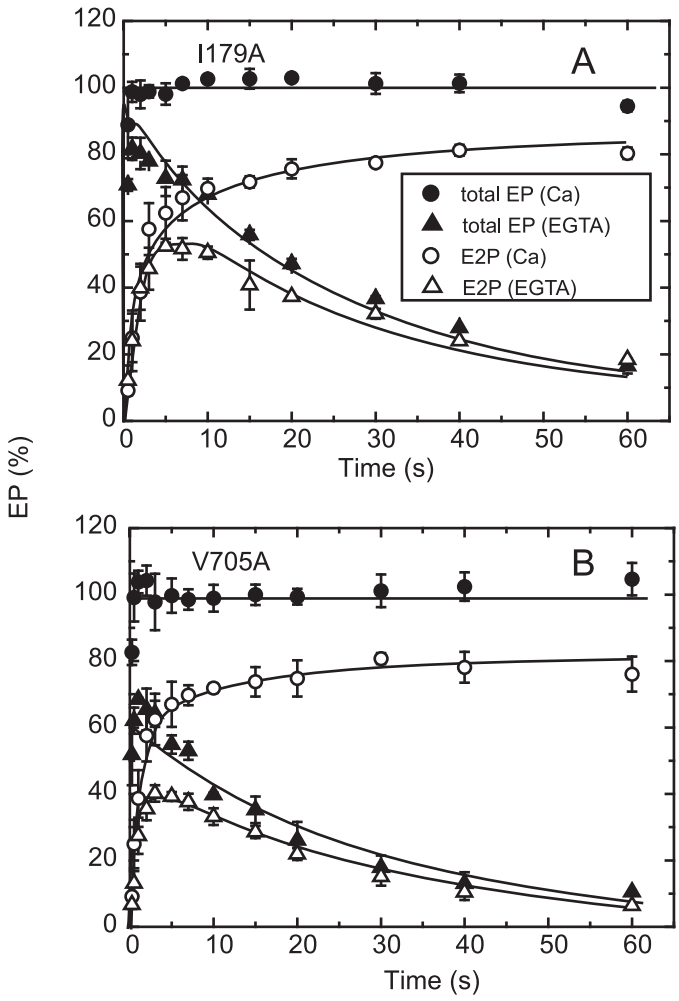

FIGURE 8. **Time courses of *EP* isomerization in mutants I179A and V705A.** The mutants I179A (*A*) and V705A (*B*) were phosphorylated with ATP, and the total amount of *E*P (*closed symbols*) and the amount of *E*2P (*open symbols*) were determined at the indicated time in an excess of EGTA (*triangles*) or in 10 μM Ca^{2+} (*circles*) as described in the *inset* in Fig. 6*B*. The fraction of *E*1P in the total amount of *E*P in the presence of 10 μM Ca^{2+} was calculated at each time point by subtracting the amount *E*2P from the total amount of *E*P (*E*1P plus *E*2P) and is depicted in Fig. 9*B*.

release. We found, with V705A (Fig. 9), that the Ca^{2+} release almost coincides with *E*2P formation, therefore the Ca^{2+} release from *E*2P is not retarded by this P domain mutation. For the mutants V726A on the P domain and I232A on the A/M3 linker, we repeatedly determined the amount of *E*2P and that of bound Ca^{2+} at a time point during the *E*P isomerization when the amount of *E*2P fraction reaches ~40–60% (Fig. 10). In both mutants, the bound Ca^{2+} and the *E*2P fraction are nearly the same, therefore there is no indication of retardation of Ca^{2+} release from *E*2P in these mutants as in V705A.

On the other hand, with mutant I179A on the A domain, Ca^{2+} release was obviously slower than the *E*P isomerization (Fig. 9); therefore, Ca^{2+} release is retarded. A curious observation with this mutant was that apparently all of the $^{45}Ca^{2+}$ is released, although ~30% of the total amount of *E*P remains as *E*1P. This again suggests that the Ca^{2+}-occluded structure of *E*1PCa_2 is partly perturbed in the mutant I179A, in this case causing a slow Ca^{2+} release. The L180A mutant does not accumulate *E*2P significantly at steady state, as found previously (18). Therefore, it was not possible to compare the kinetics of *E*2P formation and Ca^{2+} release.

Discussion

We have been able to show that several mutations at an interdomain junction at the cytoplasmic part of transmembrane helix M2 allow a separation of steps during luminal Ca^{2+} release and phosphoenzyme isomerization, steps that, in the wild type, are too fast to distinguish. This has been possible through the development of an assay that specifically measures bound, not occluded, Ca^{2+} during the release process. The difficulties in determining bound Ca^{2+} are to fix it to the protein during washing and to obtain a sufficiently high specific signal over the background, both hurdles especially acute with the

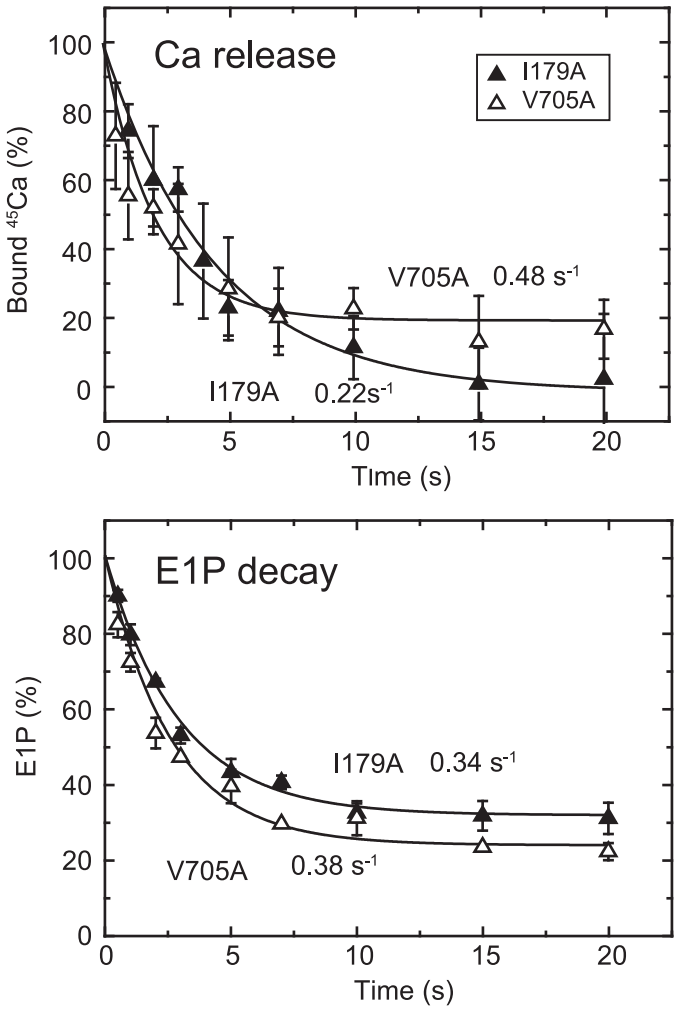

FIGURE 9. **Time courses of Ca^{2+} release and *EP* isomerization in the presence of 10 μM Ca^{2+} in mutants I179A and V705A.** *A*, Ca^{2+} release from *EP* in the mutants I179A and V705A was determined in the presence of 10 μM $^{45}Ca^{2+}$ as described in Fig. 6*A*. The values presented are the mean ± S.D. (n = 3–5). The *solid lines* show a single exponential fit, and the rates of the $^{45}Ca^{2+}$ release thus determined are 0.22 s^{-1} in I179A (*closed triangles*) and 0.48 s^{-1} in V705A (*open triangles*). *B*, the fraction of *E*1P in the total amount of *EP* was calculated at each time point in the presence of 10 μM Ca^{2+} in Fig. 8 by subtracting the amount *E*2P from the total amount of *EP* (*E*1P plus *E*2P). The values presented are the mean ± S.D. (n = 3). The *solid lines* show a single exponential fit, and the rates of the decrease in *E*1P fraction, *i.e.* the *E*1P to *E*2P isomerization, thus determined are 0.34 s^{-1} in I179A (*closed triangles*) and 0.38 s^{-1} in V705A (*open triangles*).

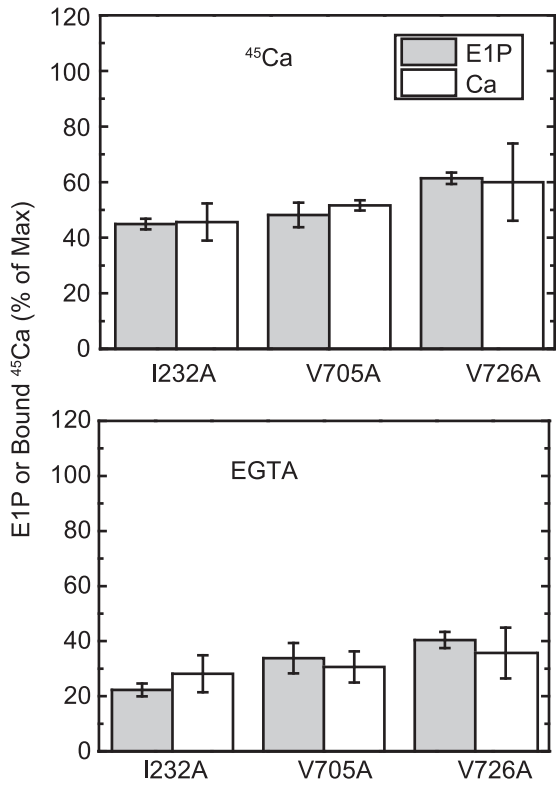

FIGURE 10. ***E*1P fraction and bound Ca^{2+}.** The amount of bound Ca^{2+} and the *E*1P fraction in total amount of *EP* (*E*1P plus *E*2P) were determined repeatedly in the presence of an excess 1 mM EGTA (*bottom panel*) or 10 μM Ca^{2+} (*top panel*) or at one selected time point during the *EP* isomerization and Ca^{2+} release time courses (*i.e.* 2 s after the start of reaction) for the mutants I232A and V726A in comparison with the mutant V705A, as described in Fig. 6. The *E*1P fraction in the total amount of *EP* and the amount of bound $^{45}Ca^{2+}$ relative to the maximum $^{45}Ca^{2+}$ binding determined at zero time are shown as indicated (*E*1P and bound ^{45}Ca, respectively). The values presented are the mean ± S.D. (n = 3–4). It should be noted that the Ca^{2+}-ATPase is dephosphorylated to the *E*2 state upon Ca^{2+} removal by an excess of EGTA (*bottom panel*) and is in all phosphorylated states in the presence of 10 μM Ca^{2+} (*top panel*, see Figs. 6–8). Therefore, there is no Ca^{2+} bound to non-phosphorylated enzyme under our experimental conditions.

small quantity of Ca^{2+}-ATPase expressed in COS-1 cell microsomes (~1% of the total protein). Our assay overcomes such problems by almost instantaneously converting the bound Ca^{2+} to a stable occluded form.

EP Isomerization with Delayed Ca^{2+} Release—In the mutants L119A and Y122A on the cytoplasmic part of M2, Ca^{2+} release in the presence of 10 μM $^{45}Ca^{2+}$ is slower than *EP* isomerization, whereas they coincide in the absence of Ca^{2+}. Retarded release in 10 μM $^{45}Ca^{2+}$ is also observed with the mutant I179A on the A domain. Such results indicate an *E*2P species with partially exchangeable Ca^{2+} that binds luminal Ca^{2+} with relatively high affinity and slowly proceeds to the Ca^{2+}-released form of *E*2P with affinity reduction. These attributes fit with our previous findings in which we analyzed luminal Ca^{2+}-induced reverse conversion of *E*2P (formed by P_i without Ca^{2+}) to *E*1PCa_2 (18) and found that the *E*2P of these mutants have luminally facing transport sites with a K_d 120–250 μM for Ca^{2+}, which is ~10 times lower than that of the wild type (K_d 1.48 mM). The kinetic analysis of the reverse conversion further indicated that the Ca^{2+} release path is not fully opened in these mutants compared with the wild type (18). It seems that, in the transient *E*2P with bound but deoccluded Ca^{2+} in the mutant L119A, Y122A, or I179A, the affinity reduction is less (K_d change from low micromolar to 120–250 μM), allowing Ca^{2+} release at moderate free Ca^{2+} concentrations.

These findings can be described by assuming a transient state **E*2P that possesses a high affinity Ca^{2+} site(s) facing the lumen (therefore, Ca^{2+} release and rebinding takes place in the presence of luminal Ca^{2+} as low as 10 μM) and proceeds to the *E*2P state with affinity reduction, as *E*1PCa_2 ↔ **E*2PCa_2 ↔ *E*2PCa_2 ↔ *E*2P + $2Ca^{2+}$. In the wild type, **E*2PCa_2 ↔ *E*2PCa_2 and subsequent Ca^{2+} ($^{45}Ca^{2+}$) release are very rapid; therefore, the **E*2P species before the affinity reduction with bound $^{45}Ca^{2+}$ is not trapped by the added non-radioactive $^{40}Ca^{2+}$. The trapping of bound $^{45}Ca^{2+}$ in the **E*2P species in the mutants L119A, Y122A, and I179A in the presence of 10 μM $^{45}Ca^{2+}$ upon addition of non-

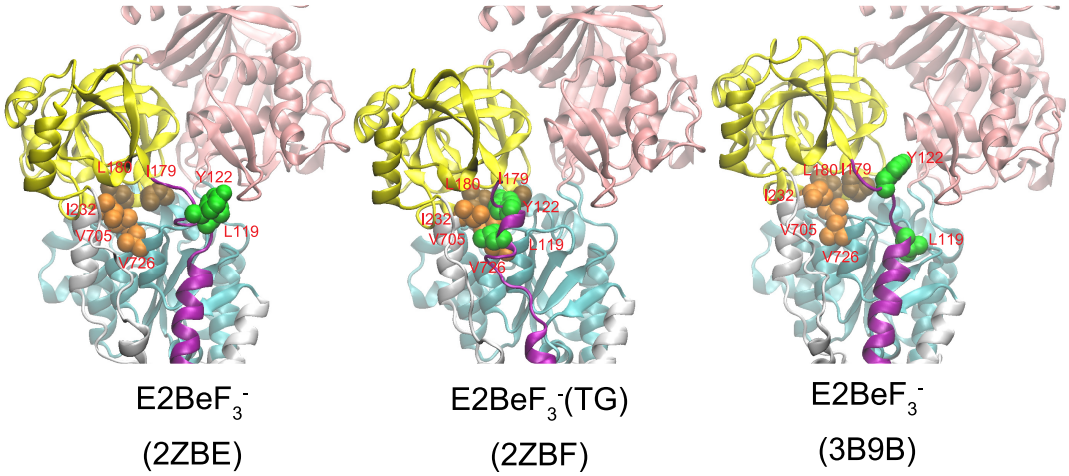

FIGURE 11. **Structures at Leu^{119}/Tyr^{122} region on the cytoplasmic part of M2 and Tyr^{122} hydrophobic cluster formation in *E2*·BeF_3^- and *E2*·BeF_3^-(TG).** The structures in *E2*·BeF_3^- (PDB codes 2ZBE (Ref. 12) and 3B9B (Ref. 13)) and in *E2*·BeF_3^-(TG) (PDB code 2ZBF (Ref. 12)) are shown as a schematic. The cytoplasmic domains A, P, and N and the cytoplasmic part of M2 are colored *yellow*, *cyan*, *pink*, and *purple*, respectively. The residues involved in the formation of Tyr^{122} hydrophobic cluster (Leu^{119}/Tyr^{122} on the cytoplasmic part of M2, Ile^{179}/Leu^{180} on the A domain, Val^{705}/Val^{726} on the P domain, and Ile^{232} on the A/M3 linker) are shown with van der Waals spheres and are colored *green* (Leu^{119}/Tyr^{122}), *brown* (Ile^{179}/Leu^{180}), and *orange* (Val^{705}/Val^{726}/Ile^{232}).

radioactive 10 mM $^{40}Ca^{2+}$ points to a possible sequential Ca^{2+} release/rebinding as $E1PCa_2 \leftrightarrow {}^*E2PCa_2 \leftrightarrow {}^*E2PCa + Ca^{2+} \leftrightarrow {}^*E2P + 2Ca^{2+} \leftrightarrow E2P + 2Ca^{2+}$, in which at least one bound $^{45}Ca^{2+}$ is trapped (as $^*E2P^{45}Ca^{40}Ca$ by $^{45}Ca^{2+}$-$^{40}Ca^{2+}$ exchange in $^*E2P$) in the reverse conversion to $E1PCa_2$ by the added 10 mM $^{40}Ca^{2+}$. Such a sequential mechanism fits with the Ca^{2+} release path in *E*2P being not fully opened in these mutants. However, it is also possible that nonspecific Ca^{2+} binding to luminal polar and negatively charged (gating) residues (43) prevents full $^{45}Ca^{2+}$ release or that Ca^{2+} substitution for Mg^{2+} at the catalytic Mg^{2+} subsite stabilizes $^*E2P$ with bound Ca^{2+}, as happens in $E1PCa_2$ (23, 26–29). Whatever the mechanism, we do not mean to imply that all bound $^{45}Ca^{2+}$ in *E*2P is fixed in the conversion to the occluded $E1PCa_2$ state but that at least some is.

Structural Rearrangements for Luminal Ca^{2+} Release during E2P Processing—In the intermediate state *E*2P with occluded Ca^{2+} ($E2PCa_2$) and its structural *E2*·BeF_3^-·Ca_2 analog trapped by elongation of the A/M1′ linker, the Leu^{119}-specific site is cleaved by proteinase K and, therefore, sterically exposed, which is in contrast to the complete resistance in the Ca^{2+}-released *E*2P ground state and its analog *E2*·BeF_3^-, formed from *E*2 in the absence of Ca^{2+} and in its TG-bound state *E2*·BeF_3^-(TG) (7, 19, 20). Evidently, some structural rearrangement takes place at the flexible Leu^{119} and Tyr^{122} region on the cytoplasmic part of M2 and Ile^{179} region on the A domain to effect Ca^{2+} deocclusion and release. Tyr^{122}/Leu^{119} on the cytoplasmic part of M2 forms a hydrophobic interaction network (Tyr^{122} hydrophobic cluster) with five other residues on the A and P domains and the A/M3 linker (Ile^{179}/Leu^{180}, Val^{705}/Val^{726}, and Ile^{232}) in *E*2P (Fig. 11), and Ile^{179} is positioned most closely to Leu^{119}/Tyr^{122} on the cytoplasmic part of M2 (Fig. 11, *2ZBE* and *3B9B*). This cluster formation has been found previously (17, 18) to be critical for the *E*2P ground state structure with potential hydrolytic activity at the catalytic site and luminally opened transport sites with reduced Ca^{2+} affinity. Therefore, the assembly of Tyr^{122}/Leu^{119} on the cytoplasmic part of M2 with the other residues and formation of the Tyr^{122} hydrophobic cluster is almost certainly accomplished during *E*2P processing to the *E*2P ground state ($E2PCa_2 \rightarrow E2P + 2Ca^{2+}$) (Fig. 12, *schematic*).

However, in the crystal structure *E2*·BeF_3^-, Leu^{119}/Tyr^{122} are not yet associated with the other five clustered residues despite being very close to Ile^{179}, which is already gathered with the other four hydrophobic residues (Leu^{180}, Val^{705}/Val^{726}, and Ile^{232}) (12, 13), whereas all seven residues are assembled in the thapsigargin-fixed structure *E2*·BeF_3^-(TG) (Fig. 11) as well as in *E2*·AlF_4^-(TG), *E2*·MgF_4^{2-}(TG), and *E2*(TG) and *E*2 (6, 9, 12, 13, 15).

Therefore, at first glance, the presently available *E2*·BeF_3^- crystal structures seem to not fit with the clustering having a critical function in the *E*2P ground state. However, it is possible that interaction of the cytoplasmic part of M2 Leu^{119}/Tyr^{122} with the A domain Ile^{179} is the final process in assembling the Tyr^{122} hydrophobic cluster, and, for some reason, it is not seen in the analog crystal structures. The cytoplasmic part of M2 in the *E*2P ground state appears rather flexible, judging from the lack of interactions here in the crystal structures, and the absence of Ca^{2+} at the transport sites may have something to do with this. We can hypothesize that even mild perturbations, such as detergent solubilization, as well as mutations here could keep the residues apart. In fact, TG binding rearranges the helices in this state to produce a tightly closed gate.

It is also of interest to note that, in our detailed analyses of the Ca^{2+} dependences of the luminal Ca^{2+}-induced reverse conversion kinetics $E2P + 2Ca^{2+} \rightarrow E1PCa_2$ and its analog *E2*·$BeF_3^- + 2Ca^{2+} \rightarrow E1Ca_2$·$BeF_3^-$, the $K_{0.5}$ of luminal Ca^{2+} was found to be 1.5 mM for *E*2P (18) and 0.4 mM for *E2*·BeF_3^- (14). Therefore, if this is not a kinetic effect, then the affinity in *E2*·BeF_3^- is somewhat higher than that for *E*2P even though *E2*·BeF_3^- seemingly possesses all of the characteristics of the *E*2P ground state; *i.e.* a hydrophobic catalytic site, the same cytoplasmic domain organization, luminally open low-affinity transport sites, and the same intrinsic tryptophan fluorescence level that reflects arrangement of the transmembrane helices. It is definitely an *E*2P ground state structural analog (7), and yet

	E1P‡Ca_2ADP	*E2P	E2P	E2P‡
	E1Ca_2·AlF_4^-·ADP (1T5T)	E2·BeF_3^- (2ZBE)	E2·BeF_3^-(TG) (2ZBF)	E2·AlF_4^-(TG) (1XP5)
Luminal Ca path	Closed	Open	Closed	Closed
Y122-HC assembling	×	Partial (only A and P)	Completed (M2 and A,P)	Completed (M2 and A,P)

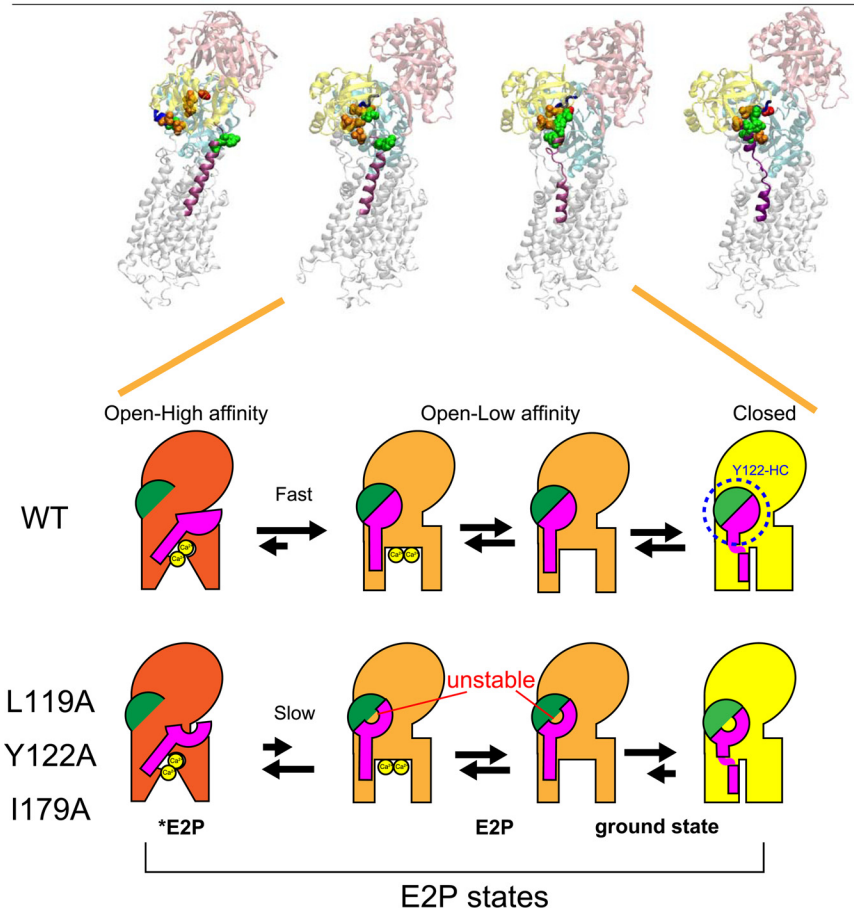

FIGURE 12. **Schematic for *E*2P processing and Ca^{2+} handling.** *Top panel*, structures of *E*1Ca_2·AlF_4^-·ADP (a structural analog for the transition state in phosphorylation, *E*1PCa_2·ADP‡, PDB code 1T5T (Ref. 10)), *E*2·BeF_3^- (PDB code 2ZBE (Ref. 12)), *E*2·BeF_3^-(TG) (PDB code 2ZBF (Ref. 12)), and *E*2·AlF_4^-(TG) ((a structural analog for the transition state in hydrolysis, *E*2P‡, PDB code 1XP5 (Ref. 11)) are shown as a schematic. In these structures, the residues involved in the formation of the Tyr^{122} hydrophobic cluster (*Y122-HC*) are depicted with van der Waals spheres and are colored as in Fig. 10 (see the residue numbers in Fig. 10). The cytoplasmic part of M2 and the $TGES^{184}$ loop are colored in *purple* and *blue*, respectively, and the A, P, and N domains are colored in *yellow*, *cyan*, and *pink*, respectively. The open or closed state of the Ca^{2+} path (luminal gate) and the assembling state of the Tyr^{122} hydrophobic cluster are indicated above the structures. *Bottom panel*, schematic of the structural changes for Tyr^{122} hydrophobic cluster formation and for the property of the Ca^{2+} transport sites and release gate during *E*2P processing with Ca^{2+} release (*E*2PCa_2 to *E*2P). In this model, the main body of Ca^{2+}-ATPase is shown in *red*, *orange*, and *yellow* to indicate the open high-affinity, open low-affinity, and closed states, respectively, for the property of the Ca^{2+} transport sites and release gate. The *green semicircle* indicates the part of Tyr^{122} hydrophobic cluster formed in *E*2PCa_2 upon *E*P isomerization (*E*1PCa_2 → *E*2PCa_2) and composed of Ile^{179}/Leu^{180} on the A domain, Val^{705}/Val^{726} on the P domain, and Ile^{232} on the A/M3 linker. The *pink structure* indicates the cytoplasmic part of M2, including Leu^{119} and Tyr^{122}. During *E*2P processing, Tyr^{122}/Leu^{119} gathers to Ile^{179} and then to the assembled five residues, completing the Tyr^{122}-hydrophobic cluster, which is coupled with affinity reduction. Mutation of Leu^{119}, Tyr^{122}, or Ile^{179} probably destabilizes the hydrophobic cluster, thereby retarding affinity reduction. Also note that our previous detailed kinetic study has revealed (18) that the *E*2P ground state structure has a closed luminal gate and that the Tyr^{122} hydrophobic cluster is tightly fixed (as described under "Discussion"), which is depicted here with a *yellow body*.

there may be subtle differences that may arise from a slight difference in the active site between the covalently bound phosphate at the catalytic aspartate (Asp^{351}) and the *E*2·BeF_3^- directly ligated with this aspartate. Alternatively, the crystallization process in detergent may impose a difference, possibly by selecting one of the putative flexible/fluctuating structures, somewhat between an "open high-affinity" state and an "open low-affinity" state. Again, we assert that the *E*2P ground state does, in fact, have a fully assembled hydrophobic cluster that completes the Ca^{2+} release process, otherwise it is difficult to explain the mutational effects.

We summarized our findings in a schematic in Fig. 12, which depicts that, after *E*P isomerization (*E*1PCa_2 → *E*2PCa_2 and loss of ADP sensitivity), the transport sites proceed from a state of open high affinity to one of open low affinity for Ca^{2+} release. The rearrangement on the cytoplasmic part of M2 (Tyr^{122}/Leu^{119}) and its assembly into a hydrophobic cluster are accomplished in this affinity reduction process by gathering of Tyr^{122}/

Leu^{119} on the cytoplasmic part of M2 with the Ile^{179}/Leu^{180} region on the A domain that is already associated with the P domain during the *E*P isomerization $E1PCa_2 \rightarrow E2PCa_2$. In the mutants L119A/Y122A and I179A, the Tyr^{122} hydrophobic cluster is destabilized, and formation of the open low-affinity state is retarded.

It is not clear why the mutations of residues Val^{705}/Val^{726} on the P domain and Ile^{232} on the A/M3 linker in the hydrophobic cluster do not retard Ca^{2+} release, but it is probably because there are several interactions between the A and P domains, and a single conservative substitution here is not enough to disrupt A-P domain association. Also, these two domains are already associated in $E2PCa_2$, and mild perturbations may be without effect on the later affinity reduction and release. There are large changes during *E*P isomerization. The A domain rotates and docks on the P domain, allowing Ile^{179}/Leu^{180} on the A domain to cluster with Val^{705}/Val^{726} on the P domain and Ile^{232} on the A/M3 linker associated with the P domain. In $E2PCa_2$, the interactions at the Val^{200} loop on the A domain with polar residues on the P domain (19, 44) and those at the $TGES^{184}$ loop on the A domain with the catalytic site on the P domain (which causes the loss of ADP sensitivity) are already produced. To effect affinity reduction and Ca^{2+} release, the associated A and P domains move together, allowing the cytoplasmic part of M2-A domain interaction at Tyr^{122}/Leu^{119} and Ile^{179} to form and complete the critical Tyr^{122} hydrophobic cluster.

Regarding a possible "closed" state in the *E*2P ground state (Fig. 12), we have found previously, with detailed kinetics in the wild type (18), that the rate of luminal Ca^{2+}-induced reverse conversion $E2P + 2Ca^{2+} \rightarrow E1PCa_2$ increases linearly with an increase in the luminal Ca^{2+} concentration and is not saturated even at 3 mM. This suggests that luminal Ca^{2+} access to the open low-affinity transport sites in *E*2P is rate-limiting, and, therefore, the gate in *E*2P may actually be closed, and the rate-limiting Ca^{2+} access may reflect opening of the closed state to an open low-affinity state. We have also found that this reverse conversion is retarded by alanine mutation of each of the seven residues in the Tyr^{122} hydrophobic cluster, and the extent of the retardation was almost the same in all seven mutants (Figs. 8 and 9 and supplemental Fig. 3 in Ref. 18). Therefore, all residues in the cluster seem important for reverse opening.

This finding (18) and the mutation-induced retardation of the forward Ca^{2+} release process found here can be accounted for by a destabilization of the open low-affinity state and transition states in the forward and reverse processes by the cluster mutations. Furthermore, the fact that all seven residues in the cluster influence the closed state implies that the change from the open low-affinity state to a tightly fixed closed state requires further rearrangements, which then permits advance to the transition state for hydrolysis (*E*2-$P^{\ddagger}$ mimicked by $E2{\cdot}AlF_4^-$), in which the gate becomes tightly closed (7).

P-type ATPases possess a common molecular structure with N, P, and A domains connected to transmembrane helices, including the long M2 helix critical for gating (1–3), and almost certainly all of them utilize a common mechanism for ion pumping. We predict that ion release to the *trans* side of the membrane will entail rearrangements at the cytoplasmic part of M2 and engagement of the A and P domains. A stepwise affinity reduction and release on this *trans* side during phosphoenzyme isomerization may be discernable even in some wild-type pumps of other P-type ATPases.

Author Contributions—K. Y. and H. S. conceived and coordinated the study and wrote the paper. K. Y. designed, performed, and analyzed the experiments. T. D. provided critical discussions and technical advice. S. D. provided technical assistance and contributed to the preparation of the figures and manuscript. All authors reviewed the results and approved the final version of the manuscript.

Acknowledgments—We thank Dr. David H. MacLennan (University of Toronto), for SERCA1a cDNA and Dr. Randal J. Kaufman (Genetics Institute, Cambridge, MA) for the expression vector pMT2. We also thank Dr. David B. McIntosh for reviewing and improving the manuscript.

References

1. Toyoshima, C. (2008) Structural aspects of ion pumping by Ca^{2+}-ATPase of sarcoplasmic reticulum. *Arch. Biochem. Biophys.* **476,** 3–11
2. Toyoshima, C. (2009) How Ca^{2+}-ATPase pumps ions across the sarcoplasmic reticulum membrane. *Biochim. Biophys. Acta* **1793,** 941–946
3. Møller, J. V., Olesen, C., Winther, A.-M. L., and Nissen, P. (2010) The sarcoplasmic Ca^{2+}-ATPase: design of a perfect chemi-osmotic pump. *Q. Rev. Biophys.* **43,** 501–566
4. Toyoshima, C., Nakasako, M., Nomura, H., and Ogawa, H. (2000) Crystal structure of the calcium pump of sarcoplasmic reticulum at 2.6 Å resolution. *Nature* **405,** 647–655
5. Danko, S., Yamasaki, K., Daiho, T., Suzuki, H., and Toyoshima, C. (2001) Organization of cytoplasmic domains of sarcoplasmic reticulum Ca^{2+}-ATPase in E_1P and E_1ATP states: a limited proteolysis study. *FEBS Lett.* **505,** 129–135
6. Toyoshima, C., and Nomura, H. (2002) Structural changes in the calcium pump accompanying the dissociation of calcium. *Nature* **418,** 605–611
7. Danko, S., Yamasaki, K., Daiho, T., and Suzuki, H. (2004) Distinct natures of beryllium fluoride-bound, aluminum fluoride-bound, and magnesium fluoride-bound stable analogues of an ADP-insensitive phosphoenzyme intermediate of sarcoplasmic reticulum Ca^{2+}-ATPase. *J. Biol. Chem.* **279,** 14991–14998
8. Toyoshima, C., and Mizutani, T. (2004) Crystal structure of the calcium pump with a bound ATP analogue. *Nature* **430,** 529–535
9. Toyoshima, C., Nomura, H., and Tsuda, T. (2004) Lumenal gating mechanism revealed in calcium pump crystal structures with phosphate analogues. *Nature* **432,** 361–368
10. Sørensen, T. L., Møller, J. V., and Nissen, P. (2004) Phosphoryl transfer and calcium ion occlusion in the calcium pump. *Science* **304,** 1672–1675
11. Olesen, C., Sørensen, T. L., Nielsen, R. C., Møller, J. V., and Nissen, P. (2004) Dephosphorylation of the calcium pump coupled to counterion occlusion. *Science* **306,** 2251–2255
12. Toyoshima, C., Norimatsu, Y., Iwasawa, S., Tsuda, T., and Ogawa, H. (2007) How processing of aspartylphosphate is coupled to lumenal gating of the ion pathway in the calcium pump. *Proc. Natl. Acad. Sci. U.S.A.* **104,** 19831–19836
13. Olesen, C., Picard, M., Winther, A. M., Gyrup, C., Morth, J. P., Oxvig, C., Møller, J. V., and Nissen, P. (2007) The structural basis of calcium transport by the calcium pump. *Nature* **450,** 1036–1042
14. Danko, S., Daiho, T., Yamasaki, K., Liu, X., and Suzuki, H. (2009) Formation of the stable structural analog of ADP-sensitive phosphoenzyme of Ca^{2+}-ATPase with occluded Ca^{2+} by beryllium fluoride. *J. Biol. Chem.* **284,** 22722–22735
15. Toyoshima, C., Iwasawa, S., Ogawa, H., Hirata, A., Tsueda, J., and Inesi, G. (2013) Crystal structures of the calcium pump and sarcolipin in the Mg^{2+}-bound E1 state. *Nature* **495,** 260–264
16. Yamasaki, K., Daiho, T., Danko, S., and Suzuki, H. (2004) Multiple and Distinct effects of mutations of Tyr^{122}, Glu^{123}, Arg^{324}, and Arg^{334} involved

in interactions between the top part of second and fourth transmembrane helices in sarcoplasmic reticulum Ca^{2+}-ATPase. *J. Biol. Chem.* **279,** 2202–2210
17. Wang, G., Yamasaki, K., Daiho, T., and Suzuki, H. (2005) Critical hydrophobic interactions between phosphorylation and actuator domains of Ca^{2+}-ATPase for hydrolysis of phosphorylated intermediate. *J. Biol. Chem.* **280,** 26508–26516
18. Yamasaki, K., Wang, G., Daiho, T., Danko, S., and Suzuki, H. (2008) Roles of Tyr^{122}-hydrophobic cluster and K^+ binding in Ca^{2+}-releasing process of ADP-insensitive phosphoenzyme of sarcoplasmic reticulum Ca^{2+}-ATPase. *J. Biol. Chem.* **283,** 29144–29155
19. Daiho, T., Yamasaki, K., Danko, S., and Suzuki, H. (2007) Critical role of Glu^{40}-Ser^{48} loop linking actuator domain and first transmembrane helix of Ca^{2+}-ATPase in Ca^{2+} deocclusion and release from ADP-insensitive phosphoenzyme. *J. Biol. Chem.* **282,** 34429–34447
20. Daiho, T., Danko, S., Yamasaki, K., and Suzuki, H. (2010) Stable structural analog of Ca^{2+}-ATPase ADP-insensitive phosphoenzyme with occluded Ca^{2+} formed by elongation of A-domain/M1′-linker and beryllium fluoride binding. *J. Biol. Chem.* **285,** 24538–24547
21. Yamada, S., and Ikemoto, N. (1980) Reaction mechanism of calcium-ATPase of sarcoplasmic reticulum. Substrates for phosphorylation reaction and back reaction, and further resolution of phosphorylated intermediates. *J. Biol. Chem.* **255,** 3108–3119
22. de Meis, L., and Inesi, G. (1982) ATP synthesis by sarcoplasmic reticulum ATPase following Ca^{2+}, PH, temperature, and water activity jumps. *J. Biol. Chem.* **257,** 1289–1294
23. Shigekawa, M., Wakabayashi, S., and Nakamura, H. (1983) Reaction mechanism of Ca^{2+}-dependent adenosine triphosphatase of sarcoplasmic reticulum. ATP hydrolysis with CaATP as a substrate and role of divalent cation. *J. Biol. Chem.* **258,** 8698–8707
24. Petithory, J. R., and Jencks, W. P. (1986) Phosphorylation of the calcium adenosinetriphosphatase of sarcoplasmic reticulum: rate-limiting conformational change followed by rapid phosphoryl transfer. *Biochemistry* **25,** 4493–4497
25. Lacapere, J. J., and Guillain, F. (1990) Reaction mechanism of Ca^{2+} ATPase of sarcoplasmic reticulum: equilibrium and transient study of phosphorylation with Ca·ATP as substrate. *J. Biol. Chem.* **265,** 8583–8589
26. Shigekawa, M., Wakabayashi, S., and Nakamura, H. (1983) Effect of divalent cation bound to the ATPase of sarcoplasmic reticulum: activation of phosphoenzyme hydrolysis by Mg^{2+}. *J. Biol. Chem.* **258,** 14157–14161
27. Wakabayashi, S., and Shigekawa, M. (1984) Role of divalent cation bound to phosphoenzyme intermediate of sarcoplasmic reticulum ATPase. *J. Biol. Chem.* **259,** 4427–4436
28. Wakabayashi, S., and Shigekawa, M. (1987) Effect of metal bound to the substrate site on calcium release from the phosphoenzyme intermediate of sarcoplasmic reticulum ATPase. *J. Biol. Chem.* **262,** 11524–11531
29. Picard, M., Jensen, A. M., Sørensen, T. L., Champeil, P., Møller, J. V., and Nissen, P. (2007) Ca^{2+} versus Mg^{2+} coordination at the nucleotide-binding site of the sarcoplasmic reticulum Ca^{2+}-ATPase. *J. Mol. Biol.* **368,** 1–7
30. Kaufman, R. J., Davies, M. V., Pathak, V. K., and Hershey, J. W. (1989) The phosphorylation state of eucaryotic initiation factor 2 alters translational efficiency of specific mRNAs. *Mol. Cell. Biol.* **9,** 946–958
31. Maruyama, K., and MacLennan, D. H. (1988) Mutation of aspartic acid-351, lysine-352, and lysine-515 alters the Ca^{2+} transport activity of the Ca^{2+}-ATPase expressed in COS-1 cells. *Proc. Natl. Acad. Sci. U.S.A.* **85,** 3314–3318
32. Weber, K., and Osborn, M. (1969) The reliability of molecular weight determinations by dodecyl sulfate-polyacrylamide gel electrophoresis. *J. Biol. Chem.* **244,** 4406–4412
33. Daiho, T., Suzuki, H., Yamasaki, K., Saino, T., and Kanazawa, T. (1999) Mutations of Arg^{198} in sarcoplasmic reticulum Ca^{2+}-ATPase cause inhibition of hydrolysis of the phosphoenzyme intermediate formed from inorganic phosphate. *FEBS Lett.* **444,** 54–58
34. Sagara, Y., and Inesi, G. (1991) Inhibition of the sarcoplasmic reticulum Ca^{2+} transport ATPase by thapsigargin at subnanomolar concentrations. *J. Biol. Chem.* **266,** 13503–13506
35. Lowry, O. H., Rosebrough, N. J., Farr, A. L., and Randall, R. J. (1951) Protein measurement with the folin phenol reagent. *J. Biol. Chem.* **193,** 265–275
36. Humphrey, W., Dalke, A., and Schulten, K. (1996) VMD: visual molecular dynamics. *J. Mol. Graph.* **14,** 33–38
37. Shigekawa, M., and Dougherty, J. P. (1978) Reaction mechanism of Ca^{2+}-dependent ATP hydrolysis by skeletal muscle sarcoplasmic reticulum in the absence of added alkali metal salts: II: kinetic properties of the phosphoenzyme formed at the steady state in high Mg^{2+} and low Ca^{2+} concentrations. *J. Biol. Chem.* **253,** 1451–1457
38. Inesi, G., Kurzmack, M., Coan, C., and Lewis, D. E. (1980) Cooperative calcium binding and ATPase activation in sarcoplasmic reticulum vesicles. *J. Biol. Chem.* **255,** 3025–3031
39. Inesi, G. (1987) Sequential mechanism of calcium binding and translocation in sarcoplasmic reticulum adenosine triphosphatase. *J. Biol. Chem.* **262,** 16338–16342
40. Petithory, J. R., and Jencks, W. P. (1988) Binding of Ca^{2+} to the calcium adenosinetriphosphatase of sarcoplasmic reticulum. *Biochemistry* **27,** 8626–8635
41. Orlowski, S., and Champeil, P. (1991) Kinetics of calcium dissociation from its high-affinity transport sites on sarcoplasmic reticulum ATPase. *Biochemistry* **30,** 352–361
42. Yamasaki K, Daiho T, Danko S, and Suzuki H. (2010) Ca^{2+} release to lumen from ADP-sensitive phosphoenzyme $E1PCa_2$ without bound K^+ of sarcoplasmic reticulum Ca^{2+}-ATPase. *J. Biol. Chem.* **285,** 38674–38683
43. Webb, R. J., Khan, Y. M., East, J. M., and Lee, A. G. (2000) The importance of carboxyl groups on the lumenal side of the membrane for the function of the Ca^{2+}-ATPase of sarcoplasmic reticulum. *J. Biol. Chem.* **275,** 977–982
44. Kato, S., Kamidochi, M., Daiho, T., Yamasaki, K., Gouli, W., and Suzuki, H. (2003) Val^{200} residue in Lys^{189}-Lys^{205} outermost loop on the A domain of sarcoplasmic reticulum Ca^{2+}-ATPase is critical for rapid processing of phosphoenzyme intermediate after loss of ADP sensitivity. *J. Biol. Chem.* **278,** 9624–9629
45. Barrabin, H., Scofano, H. M., and Inesi, G. (1984) Adenosinetriphosphatase site stoichiometry in sarcoplasmic reticulum vesicles and purified enzyme. *Biochemistry* **23,** 1542–1548